

Polymeric nanoparticle-based mRNA vaccine is protective against influenza virus infection in ferrets

Gijs Hardenberg,¹ Chantal Brouwer,¹ Rachele van Gemerden,¹ Nicola J. Jones,² Anthony C. Marriott,² and Jaap Rip¹

¹20Med Therapeutics BV, Galileiweg 8, 2333BD Leiden, the Netherlands; ²UK Health Security Agency, Porton Down, SP4 0JG Salisbury, UK

New therapies and vaccines based on nucleic acids combined with an efficient nanoparticle delivery vehicle have a broad applicability for different disease indications. An alternative delivery technology for the successfully applied lipid nanoparticles in mRNA SARS-CoV-2 vaccines are nanoparticles composed of biodegradable poly(amido)amine-based polymers with mRNA payload. To show that these polymeric nanoparticles can efficiently deliver influenza hemagglutinin mRNA to target tissues and elicit protective immune responses, a relevant ferret influenza challenge model was used. In this model, our nanoparticle-based vaccine elicited strong humoral and cellular immune responses in the absence of local and systemic reactogenicity. Upon virus challenge, vaccinated animals exhibited reduced clinical signs and virus load relative to unvaccinated control animals. Based on these findings, further investigation of the polymeric nanoparticles in the context of prophylactic vaccination is warranted. Future studies will focus on optimizing the payload, the nanoparticle stability, the efficacy in the context of pre-existing immunity, and the applicability of the technology to prevent other infectious diseases.

INTRODUCTION

With an estimated 290,000–650,000 deaths each year from seasonal influenza,¹ yearly changing circulating strains, and the pandemic risks associated, influenza forms the next logical target for mRNA vaccines. By circumventing the need for time-consuming egg adaptations that are associated with egg-based vaccine production, vaccine strains could be selected closer to the actual season, potentially avoiding wrong strain predictions and egg-based mismatches resulting in more efficacious seasonal influenza vaccines that can pave the way for a rapid pandemic rollout if needed. Instead of relying on heavily patented lipid nanoparticle (LNP) technology that requires an ultra-cold chain for transport and storage and is associated with reactogenicity, we here present poly(amido)amine-based polymeric nanoparticles (NPs) as an alternative mRNA vaccine technology that is easy to manufacture and scale up with a favorable preclinical reactogenicity profile.

Poly(amido)amine (PAA)-based polymeric nanoparticles (ps-PAAQ NP) can be used for efficient *in vitro* and *in vivo* mRNA delivery and cell transfection.² The ps-PAAQ polymers are synthesized using a

polymerization reaction that differentiates them from the recently reviewed and more commonly used PAA dendrimers.³ The technology consists of a combination of biodegradable polymers that can be mixed with different nucleic acid-based payloads to form NPs of uniform size. Since the formulation is made in an all-aqueous solution with an mRNA encapsulation efficiency of >95%, no further purification step is needed, which avoids loss of material and maximizes yield. In this study, we show for the first time the successful use of this alternative delivery technology applied in an mRNA vaccine.

To show that the use of this technology in mRNA vaccines elicits protective immune responses, modified mRNA expressing influenza hemagglutinin (HA) was encapsulated in the NPs and tested in a ferret influenza challenge model. Ferrets are considered a suitable model for human influenza research as their respiratory tract resembles that of humans and they are susceptible to unadapted human influenza viruses.⁴ HA is a major antigenic determinant in commercial influenza vaccines and it is well established that antibodies to HA can reduce influenza-related morbidity and mortality.⁵ T cell responses against HA play an important role in viral clearance and heterosubtypic immunity in humans and animal models^{6,7} and vaccines that allow for their induction are generally preferred.

In this study we used polymeric ps-PAAQ NPs with mRNA HA as an influenza vaccine in a ferret viral challenge model. For the *in vivo* study we used a prime and boost vaccination followed by analysis of the immune response. The study design included an HAI titration-based go/no-go criterium before moving to the viral challenge phase.

RESULTS

Study design

Three weeks after bleeding ferrets for pre-existing antibody screening and to obtain baseline peripheral blood mononuclear cells (PBMCs), ferrets were vaccinated (day 0). One group of six ferrets (four males and two females) was immunized intramuscularly with 30 µg HA-Cal09 mRNA

Received 25 October 2023; accepted 15 February 2024;
<https://doi.org/10.1016/j.omtn.2024.102159>.

Correspondence: Jaap Rip, 20Med Therapeutics BV, Galileiweg 8, 2333BD Leiden, the Netherlands.

E-mail: rip@20medtx.com



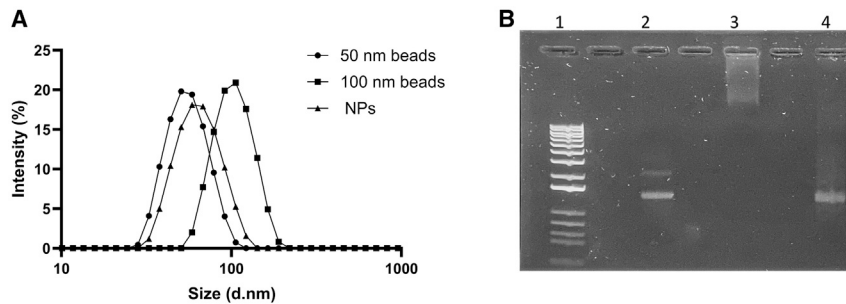


Figure 1. NP size and mRNA encapsulation

(A) Nanoparticle size distribution measurement with DLS and shown as signal intensity. Polystyrene beads with an average size of 50 and 100 nm were used as references. The average size of the vaccine nanoparticles was 61 nm with a polydispersity index of 0.07. (B) Agarose gel with a DNA ladder (lane 1), mRNA Cal09 (lane 2), mRNA Cal09 in NPs (lane 3), and mRNA Cal09 released from NPs with DTT/heparin (lane 4).

in ps-PAAQ NPs (group A). The control group included six ferrets (four males and two females) and was intramuscularly injected with buffer (group B). Animals were bled again for PBMCs and serum on day 18. This was followed by a homologous boost immunization or a repeat injection with buffer on day 20. In [Figure S4](#), a graphical representation of the treatment schedule is provided.

NP formulation and characterization

NPs were formulated using N1-methyl-pseudo-Uridine modified mRNA expressing HA from influenza Cal09 as payload. Cal09 was the initial vaccine virus to combat the H1N1 pandemic influenza virus that emerged in 2009.⁸

Prior to *in vivo* efficacy testing, essential NP characteristics (such as size, charge, and encapsulation efficiency) were determined. The average size of the NPs was 61 nm with a polydispersity index of 0.07 ([Figure 1A](#)) and a zeta potential of -3.7 mV. Encapsulation of mRNA in the NPs was confirmed using agarose gel electrophoresis with no “free” mRNA visible indicating full encapsulation of mRNA starting material ([Figure 1B](#)). Endotoxin levels were determined to be below 0.3 EU/animal in a Bacterial Endotoxin/Turbidimetric Kinetic LAL test. The functionality of the mRNA construct was confirmed by *in vitro* transfection of HEK293T cells with the NPs and HA antigen expression confirmed in the cell lysates.

Reactogenicity and immunogenicity

No local reactogenicity (e.g., swelling) was observed following vaccination or injection with buffer and no systemic reactions (e.g., body weight loss or temperature changes) were observed following primary or booster vaccination ([Figure S5](#)).

Animals were followed up for the development of serum HAI titers and neutralizing antibodies against GM19. HAI titers were readily induced in all vaccinated animals after the prime immunization and further increased (on average 2.7-fold) after the boost. Buffer control-injected animals remained HAI-negative until after the virus challenge described below ([Figure 2A](#)).

To confirm serum HAI titers were also induced against the vaccine virus, we measured HAI titers against A/California/07/09 after the boost and found HAI titers ≥ 256 in four of six ferrets ([Figure 2B](#)).

Furthermore, we could show that sera from vaccinated animals had neutralizing activity against GM19 and this neutralizing activity increased (on average 3.7-fold) after the homologous boost immunization ([Figure 2C](#)).

In line with the HAI and virus neutralizing antibody responses, we observed T cell responses to Cal09 (H1N1) virus and Cal09 (H1N1) HA peptides in interferon-gamma (IFN- γ) ELISpot after prime immunization, which further increased after boost immunization ([Figure 3](#)).

Virus challenge

After the viral challenge, mild weight loss was observed in both vaccinated and buffer-treated animals with a mean peak weight loss for vaccinated animals of 4.74% compared with 6.39% for the buffer group ([Figure 4](#)). When weight loss was assessed by calculating the area under the curve (AUC) of each individual animal, there was no significant difference between the groups (2-tailed t test with Welch’s correction, $p = 0.41$). In addition, maximum % weight loss during the 14 days post infection was calculated for each animal and ranged from 2.8% to 8.8%, with no significant difference between the groups (2-tailed t test, $p = 0.18$).

For each ferret, twice-daily observations were made for clinical signs such as sneezing, nasal discharge, labored breathing, and inactivity, covering the 14 days post challenge. Clinical signs were significantly decreased in vaccinated animals ([Figure 5A](#)), with labored breathing, generally considered a much more severe clinical symptom,⁹ only observed in buffer-treated animals ([Figure S3](#)).

Furthermore, we observed a significant difference in core body temperature between vaccinated and buffer-treated animals, with buffer-treated animals showing elevated temperatures as determined by AUC analysis of temperature change in vaccinated animals compared with the buffer group ($p = 0.039$, [Figure 5B](#)). The body temperature change was calculated by subtracting the baseline temperature for each ferret. In both groups, we observed a disruption to the diurnal rhythm seen prior to infection, with normal cycling resuming approximately 170 h (7 days) post infection ([Figure S1](#)).

Nasal wash cell counts showed a rise from baseline between 1 and 2 days post infection (dpi) but did not differ between both treatment groups

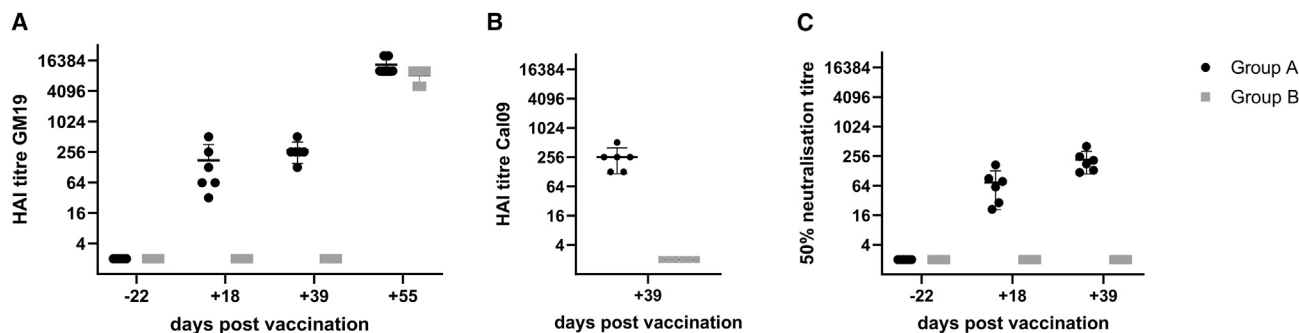


Figure 2. HAI and microneutralization titers

(A) Hemagglutination inhibition (HAI) titers of group A and group B ferrets to A/Guangdong-Maonan/SWL1536/2019 H1N1 (GM19) virus at baseline (day -22), post prime (day 18), post boost (day 39), and after challenge (day 55, 2 weeks post challenge). Points represent individual ferret sera; lines show mean and standard deviation. Titers of <4 are plotted as 2. (B) HAI titers of group A and group B ferrets to A/California/07/09 virus post boost (day 39). Points represent individual ferret sera; lines show mean and standard deviation. Titers of <8 are plotted as 2. (C) Serum microneutralization titers to H1N1 virus in group A and group B ferrets at baseline (pre-vaccine, day -22), post prime (day 18), post boost (day 39). Sera were tested for neutralizing antibodies against GM19 using a focus-reduction assay. Points represent individual ferret sera and lines show mean and standard deviation from each group. Endpoints are expressed as the titer giving a 50% reduction of viral foci. Titers of <4 or where the data could not be fit to a sigmoidal curve are plotted as 2.

(Figure S2), whereas mean nasal wash viral titers in vaccinated animals were significantly lower than buffer-treated animals 2, 3, 5, 6, and 7 dpi (p values: 2 dpi p = 0.00096; 3 dpi p = 0.021; 5 dpi p = 0.011; 6 dpi p = 2.2×10^{-6} ; 7 dpi p = 4.0×10^{-7}) (Figure 6A). These findings were further substantiated by significantly higher AUC nasal wash virus titers, which represent the total virus shed by each ferret, in buffer-treated animals compared with ps-PAAQ NP HA-Cal09-vaccinated animals (p < 0.0001, Figure 6B) and the finding that ferrets in the buffer-treated group shed virus in nasal wash approximately 2 days longer than vaccinated ferrets. No virus was detectable in nasal washes from vaccinated animals from 6 dpi onward, whereas two of six ferrets in the buffer-treated group still showed detectable virus 8 dpi (Figure 6A).

DISCUSSION

We tested ps-PAAQ NPs as mRNA delivery technology applied in an influenza vaccine. A strong humoral and cellular immune response was found with no local or systemic reactogenicity of the vaccination in the ferrets. Upon virus challenge, vaccinated animals exhibited reduced clinical signs and virus load relative to the buffer-injected control animals.

In this study, we found that all ferrets responded to the vaccine by 18 d post vaccination as measured by HAI titers against GM19 (≥ 4 -fold increase from baseline) and three of six ferrets showed a further ≥ 4 -fold increase in HAI titer following the booster vaccination resulting in HAI titers ≥ 256 in five of six ferrets. Additionally, we observed strong virus and HA-specific T cell responses after prime and boost immunization (means >100 SFU/10⁶ cells for both stimuli after boost), reduced nasal virus load, and protection against severe disease. Although not directly compared in this current study, these results clearly differ from the response and degree of protection reported by Cheng et al.⁷ and others^{10,11} after trivalent inactivated influenza vaccine (TIV) immunization in ferrets.^{7,12} In the study from Cheng et al.,⁷ naive ferrets responded poorly to TIV, with barely detectable HAI antibody titers to all three strains, and this resulted in poor protection against a heterologous H1N1 challenge with no virus reduction in nose and lungs.^{13,14} Pre-exposure of ferrets to influenza virus, however, greatly improved efficacy of TIV immunization in a different study.¹⁵ Previous work using a different polymeric NP approach in combination with self-amplifying RNA encoding for HA-Cal09 by Shattock et al. resulted in 50% of ferrets in the high-dose (80 μ g) group seroconverting in HAI and variable levels of protection against a

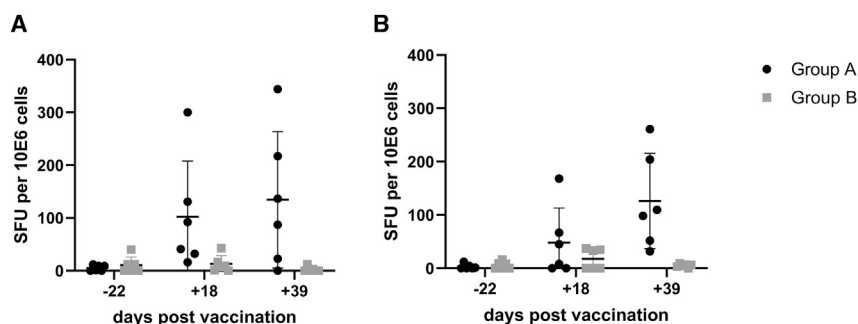


Figure 3. T cells

Cellular immune response of ferrets in group A and group B after prime and boost. T cell responses were assessed by interferon (IFN)- γ ELISpot on PBMC at baseline (day -22), post prime (day 18), and post boost (day 39). Points represent individual ferret PBMCs, and lines show mean and standard deviation from each group. (A) The results of stimulation with A/California/07/09 HA peptides. (B) The results of stimulation with whole A/California/07/09 virus.

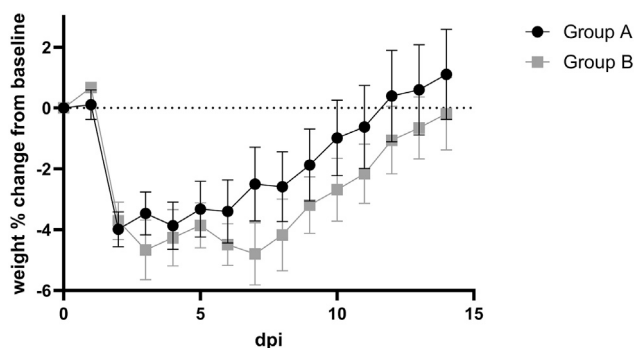


Figure 4. Animal weight change

Weight percentage change from baseline between days 0 and 14 post challenge in group A and group B ferrets. Lines show group means \pm SEM. dpi = days post infection.

homologous infection,¹⁶ whereas all ferrets seroconverted in HAI at 30 μ g mRNA dose in our hands and were protected against severe disease. More promising immunogenicity and efficacy results were obtained with LNP-based mRNA vaccines in ferrets. These studies differ from our study by the delivery technology used and also by the use of self-amplifying RNA or multiple influenza antigens making a direct comparison difficult.^{10,11,17,18} The current generation of LNP vaccines is not yet optimal with regard to vaccine storage conditions and reactogenicity. They require ultra-cold storage and their reactogenicity exceeds the reactogenicity observed for conventional influenza vaccines. For example, 70% of recipients experienced adverse reactions (pain, swelling at injection site, headache, myalgia, and fatigue) in a recent clinical trial of the mRNA-based seasonal influenza vaccine (mRNA-1010).¹⁹ Despite the reported inherent variability in response to influenza infection in ferrets²⁰ we observed improved virus clearance and alleviation of disease symptoms in naive ferrets without adverse events (injection site observations, weight loss, and fever) when using a polymeric NP-based HA vaccine.

Advantages of the polymeric ps-PAAQ NPs include the possibility to carry different types of nucleic acids, the adaptability and ease of the

formulation process, and the ability to be lyophilized, making them an attractive alternative for various medical applications. The same approach and technology can be used for the development of multi-valent mRNA vaccines. A mixture of different mRNA constructs encoding different influenza strain-specific antigens can be loaded in a single step in the NPs. We have used a single formulation of NPs to successfully express different (reporter) proteins after *in vitro* transfection of cells (data not shown). The one-step formulation of the NPs without the need for further purification avoids loss of materials and allows for fast, local, and bedside preparations that can be advantageous for personalized medicine applications. The uniform NP size and the possibility to maintain the NP characteristics after freeze-thawing and lyophilization enables long-term shelf-life stability. This is important for medical applications, as it allows for stockpiling and distribution of ready-to-use formulations.

The results of this study warrant further development of our platform in the context of mRNA vaccines. Future studies will focus on optimizing the payload (and the possibility to include multiple antigens), NP stability, and testing the vaccine in heterologous challenge models and in the context of pre-existing immunity.

MATERIALS AND METHODS

Polymer synthesis and NP formulation

Poly(amido)amine polymers were synthesized as described (ps-PAAQ, Münzebrock et al.²¹). In short, cystamine bis(acrylamide) (CBA) was synthesized as described by Lin et al.²² and N1-(7-chloroquinolin-4-yl)-hexane-1,6-diamine (Q6), was synthesized as described by Natara-jan et al.²³ The ps-PAAQ (or p(CBA-ABOL-Q)/PEI) was synthesized by Michael-type polymerization of primary amines with bis-acrylamides.²³ A small round-bottom flask was charged with 4-aminobutanol (ABOL) (0.60 g, 6.73 mmol), bis(acrylamide) (CBA) (2.60 g, 10 mmol), and N1-(7-chloroquinolin-4-yl)-hexane-1,6-diamine (Q6) (0.60 g, 2.16 mmol). MeOH (10 mL) was added, followed by a solution of CaCl₂ (0.44 g, 4 mmol) in water (2 mL). The resulting suspension was heated to 50°C and incubated for 48 h while stirring. A solution of branched PEI800 (Sigma-Aldrich Mn 600, 100 mg/mL in water, 680 μ L) was then added and the reaction mixture was allowed to stir

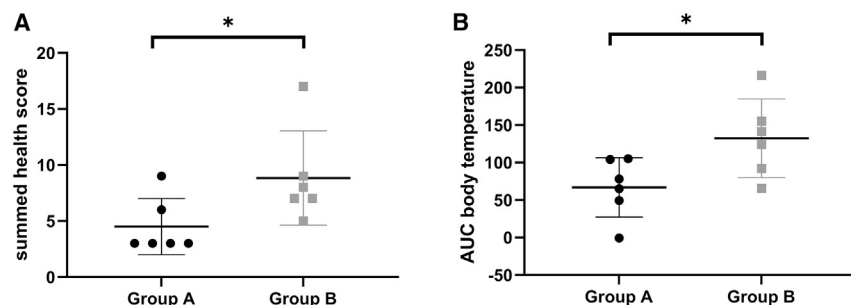


Figure 5. Summed health score and body temperature

(A) For each ferret between days 0 and 14 post challenge, clinical signs and activity levels were recorded twice daily. A score of 0 or 1 was assigned for the absence or presence, respectively, of the following clinical signs: diarrhea; nasal discharge; nasal congestion/mouth breathing; nasal rattles/sneezing; labored breathing. Activity levels were assessed and assigned the following scores: 0 = alert and playful; 1 = alert and playful when stimulated; 2 = alert but not playful when stimulated; 3 = not alert or playful. All scores were summed for each ferret over the period of

observation and plotted. Points represent individual ferrets and lines show median with interquartile range from each group. Vaccinated animals (group A) showed significantly lower scores than buffer-treated animals (group B) (Mann-Whitney test, 2-tailed, * $p = 0.048$). (B) The area under the curve (AUC) body temperature was calculated for each ferret. Points represent individual ferret data and lines show mean and standard deviation from each group. Buffer-treated animals (group B) showed a significantly higher AUC body temperature than ps-PAAQ NP HA-Cal09-vaccinated animals (group A) (2-tailed t test with Welch's correction, * $p = 0.039$).

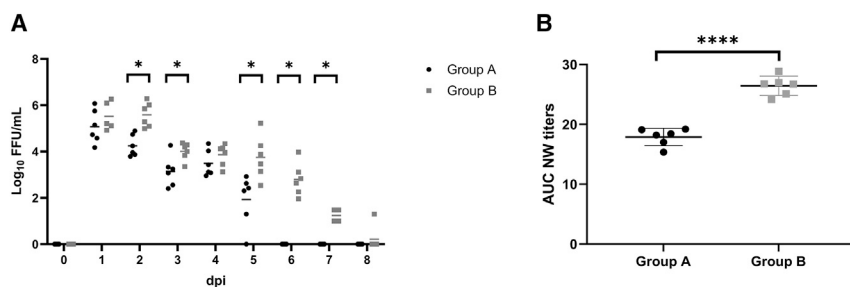


Figure 6. AUC nasal wash virus titers

(A) Nasal washes were collected 2 days prior to challenge and for 8 days post challenge to measure nasal wash virus titers. Viral titers were measured using the focus-forming unit (FFU) assay (ViroSpot). Data were log-transformed for plotting; titers of zero were set at 1 FFU/mL to allow plotting. Individual animals are depicted with symbols, and lines show means. Groups were compared by multiple t tests, and significant differences were seen on the days marked *. dpi = days post infection. (B) The area under the curve (AUC) nasal wash virus titer was calculated for each

ferret. Lines show mean and standard deviation from each group. The AUC nasal wash virus titer of vaccinated animals (group A) was significantly less than the AUC nasal wash virus titer from the buffer-injected group (group B) (unpaired 2-tailed t test, ****p < 0.0001).

for another 72 h with heating and stirring. The reaction was acidified to pH 4 with hydrochloric acid and dialyzed against water. The material was filtered through a 0.45- μ m filter (cellulose acetate) and lyophilized to yield the ps-PAAQ polymer as a (hygroscopic) white solid.

A second polymer PEG-PGA (12.5 kDa) was synthesized by ring opening polymerization of *O'*-benzyl-L-glutamic acid N-carboxyanhydride initiated by mPEG-amine (5 kDa). Deprotection was performed using HBr in TFA. After workup and subsequent neutralization with sodium hydroxide, purification with TFF was performed yielding the sodium salt of PEG-PGA with a degree of polymerization of 50 as assayed by NMR.

mRNA encoding influenza A California 07/2009 (Cal09) HA (H1N1) was synthesized by Trilink with CleanCap reagent and the modified NTP, N1-Methyl-Pseudo-U. NPs were formed by mixing a 0.3 mg/mL solution of mRNA encoding Cal09 HA in 8% trehalose, 10 mM histidine, 7.5 mg/mL PEG-PGA at pH 6.5 with a 7.5 mg/mL solution of ps-PAAQ polymers in 8% trehalose, 10 mM histidine buffer at pH 6.5 in a 1:1 (v/v) ratio using a syringe pump. After incubating 30 min at room temperature (RT), resulting NPs were aliquoted in 2 mL – 2R glass vials and stored at -80°C until use.

NP characterization

Cal09 HA mRNA containing NPs were characterized (size, zeta potential, and polydispersity) using dynamic light scattering (DLS) in the Zetasizer Nano ZS90 (Malvern). mRNA encapsulation, heparin/DTT-mediated release, and identity were confirmed with gel electrophoresis and *in vitro* HA expression was confirmed in H1 ELISA on lysates of NP-transfected HEK293T cells.

Animals

Ferrets (*Mustela putorius furo*) (8–11 weeks old, eight males and four females) were obtained from Marshall Bioresources, UK, and confirmed as seronegative for influenza A, B, and GM19 virus. Since there were not a sufficient number of female ferrets available to use an equal mixture in each group, the same proportion of male to female was used instead.

Mean weight at vaccination was 452 g for female ferrets and 802 g for male ferrets. Each animal was individually identified by an identifier/thermal chip implanted subcutaneously in each animal's side on day –22 (day 0 is prime vaccination). In addition, on day –16, Star-Oddi

DST nano-T temperature loggers were implanted subcutaneously (nape of neck) to measure fluctuations in body temperature during the study. The health and welfare of the animals were monitored each day. Additional weight and temperature checks were done between 2 days prior and after each vaccination combined with monitoring for adverse reactions on the day of vaccination and twice daily for 2 days after.

Vaccination was composed of 0.2 mL ps-PAAQ NP formulation containing 30 μ g mRNA divided over the rear right and left quadriceps femoris muscle. Control animals received intramuscular buffer injections.

For the viral challenge, animals were sedated with isoflurane prior to intranasal instillation of virus (0.2 mL total, 0.1 mL per nostril) diluted in phosphate-buffered saline (PBS). Virus challenge was performed by intranasal inoculation of a high dose (1×10^6 PFU) of A/Guangdong-Maonan/SWL1536/2019 H1N1 (GM19) virus (egg passage P + E5). This virus strain is close to Cal09 in amino acid sequence (95.9% sequence identity) but has clear differences in sites known to be immunodominant in ferrets: Sa, Sb, Ca, and Cb²⁴ (Figure 7).²⁵ The challenge dose was confirmed on day of administration by back-titration of the inoculum in a ViroSpot assay. Virus replication in the upper respiratory tract was measured by virus load determination in consecutively collected nasal washes. For nasal washes, ferrets were anesthetized using isoflurane and 2 mL (1 mL/nare) of PBS (Gibco, Loughborough, UK) was administered intranasally and used to lavage the nasal cavity. In addition, to monitor the inflammatory immune response in the nasal cavity, nasal wash cell counts were determined. From the day of challenge onward, twice-daily clinical observations and activity assessments were performed, daily weight measurements were taken, and hourly temperature logging started.

Blood samples were taken at various timepoints from the cranial vena-cava vessel of ferrets using a needle and syringe into either BD Vacutainer Heparin Blood Collection tubes for PBMC collection or BD Vacutainer SST tubes for serum collection. Blood taken for serum was left to clot at RT for at least 30 min. The tubes were then placed into a centrifuge a spun at $1,000 \times g$ for 10 min to separate serum. Serum was removed and aliquoted into cryovials (Nunc,

Interferon-gamma ELISpot

PBMCs were assessed for responses to Cal09 virus and HA Peptivator peptides (derived from Cal09 virus; Miltenyi Biotech). Following overnight stimulation, IFN- γ expressing cells were detected using the ferret IFN- γ ELISpot kit with pre-coated plates (Mabtech, Nacka, Sweden). Results from duplicate tests were averaged. Data were analyzed by subtracting the mean number of spots in the control wells (cells only) from the mean counts of spots in wells with cells and antigen.

Virological readouts

Virosport assay

MDCK-SIAT1 cells were seeded in 96-well plates overnight, washed with PBS, and incubated with 10-fold serial sample dilutions in serum-free media (DMEM). After 1 h at 37°C, sample dilutions were carefully removed and 100 μ L overlay media containing 1% CMC and 1/150 volume TrypLE Select (Gibco) was added to each well. After incubation for 17–22 h at 37°C, the overlay was removed and the plates were fixed with 100% ice-cold methanol for a minimum of 15 min. Plates were washed with PBS, and 50 μ L per well mouse monoclonal anti-influenza NP (clone AA5H) at 1:1,000 was added for 1 h at RT. Plates were again washed with PBS, and 50 μ L goat anti-mouse IgG-alkaline phosphatase at 1:1,500 was added for 1 h at RT. Plates were washed with PBS, and 50 μ L filtered substrate (NBT/BCIP) was added until spots developed (~30 min). Plates were washed with water and once dry, analyzed using a CTL scanner and software (CTL, Germany).

DATA AND CODE AVAILABILITY

All data are included in the paper and its [supplemental information](#). Materials and access to raw data will be supplied by the authors upon reasonable request.

SUPPLEMENTAL INFORMATION

Supplemental information can be found online at <https://doi.org/10.1016/j.omtn.2024.102159>.

ACKNOWLEDGMENTS

Design of mRNA encoding Cal09 HA was supported by Touchlight Genetics Ltd. This study has been carried out with financial support from Horizon 2020 Framework Programme grant number 730694 (TRANSVAC2).

AUTHOR CONTRIBUTIONS

J.R. and A.M.: Conceptualization, Methodology. G.H.: Writing - Original draft preparation, visualization. N.J., A.M., C.B., and R.G.: Investigation. J.R. and A.M.: Supervision. A.M.: Validation. J.R. and A.M.: Writing - Reviewing and Editing.

DECLARATION OF INTERESTS

J.R., G.H., C.B., and R.G. are employees of 20Med Therapeutics.

REFERENCES

1. Paget, J., Spreeuwenberg, P., Charu, V., Taylor, R.J., Iuliano, A.D., Bresee, J., Simonsen, L., and Viboud, C.; Global Seasonal Influenza-associated Mortality Collaborator Network and GLaMOR Collaborating Teams* (2019). Global mortality associated with seasonal influenza epidemics: New burden estimates and predictors from the GLaMOR Project. *J. Glob. Health* 9, 020421.
2. Pontes, A.P., Welting, T.J.M., Rip, J., and Creemers, L.B. (2022). Polymeric Nanoparticles for Drug Delivery in Osteoarthritis. *Pharmaceutics* 14, 2639.
3. Kisakova, L.A., Apartsin, E.K., Nizolenko, L.F., and Karpenko, L.I. (2023). Dendrimer-Mediated Delivery of DNA and RNA Vaccines. *Pharmaceutics* 15, 1106.
4. Maher, J.A., and DeStefano, J. (2004). The ferret: An animal model to study influenza virus. *Lab Anim.* 33, 50–53.
5. Gallagher, J.R., McCraw, D.M., Torian, U., Gulati, N.M., Myers, M.L., Conlon, M.T., and Harris, A.K. (2018). Characterization of hemagglutinin antigens on influenza virus and within vaccines using electron microscopy. *Vaccines (Basel)* 6, 31.
6. Sridhar, S. (2016). Heterosubtypic T-cell immunity to influenza in humans: Challenges for universal T-cell influenza vaccines. *Front. Immunol.* 7, 195.
7. Cheng, X., Zengel, J.R., Suguitan, A.L., Xu, Q., Wang, W., Lin, J., and Jin, H. (2013). Evaluation of the humoral and cellular immune responses elicited by the live attenuated and inactivated influenza vaccines and their roles in heterologous protection in ferrets. *J. Infect. Dis.* 208, 594–602.
8. Sullivan, S.J., Jacobson, R.M., Dowdle, W.R., and Poland, G.A. (2010). 2009 H1N1 influenza. *Mayo Clin. Proc.* 85, 64–76.
9. Moncla, L.H., Ross, T.M., Dinis, J.M., Weinfurter, J.T., Mortimer, T.D., Schultz-Darken, N., Brunner, K., Capuano, S.V., 3rd, Boettcher, C., Post, J., et al. (2013). A novel nonhuman primate model for influenza transmission. *PLoS One* 8, e78750.
10. Chang, C., Music, N., Cheung, M., Rossignol, E., Bedi, S., Patel, H., Safari, M., Lee, C., Otten, G.R., Settembre, E.C., et al. (2022). Self-amplifying mRNA bicistronic influenza vaccines raise cross-reactive immune responses in mice and prevent infection in ferrets. *Mol. Ther. Methods Clin. Dev.* 27, 195–205.
11. van de Ven, K., Lanfermeijer, J., van Dijken, H., Muramatsu, H., Vilas Boas de Melo, C., Lenz, S., Peters, F., Beattie, M.B., Lin, P.J.C., Ferreira, J.A., et al. (2022). A universal influenza mRNA vaccine candidate boosts T cell responses and reduces zoonotic influenza virus disease in ferrets. *Sci. Adv.* 8, ead9937.
12. Skowronski, D.M., Hamelin, M.E., De Serres, G., Janjua, N.Z., Li, G., Sabaiduc, S., Bouhy, X., Couture, C., Leung, A., Kobasa, D., et al. (2014). Randomized controlled ferret study to assess the direct impact of 2008-09 trivalent inactivated influenza vaccine on A(H1N1)pdm09 disease risk. *PLoS One* 9, e86555.
13. Houser, K.V., Katz, J.M., and Tumpey, T.M. (2013). Seasonal Trivalent Inactivated Influenza Vaccine Does Not Protect against Newly Emerging Variants of Influenza A (H3N2v) Virus in Ferrets. *J. Virol.* 87, 1261–1263.
14. Music, N., Reber, A.J., Lipatov, A.S., Kamal, R.P., Blanchfield, K., Wilson, J.R., Donis, R.O., Katz, J.M., and York, I.A. (2014). Influenza vaccination accelerates recovery of ferrets from lymphopenia. *PLoS One* 9, e100926.
15. Francis M.E., McNeil M., King M.L., Ross T.M., Kelvin A.A. Influenza Preimmunity Increases Vaccination Efficacy by Influencing Antibody Longevity, Neutralization Activity, and Epitope Specificity. Preprint at bioRxiv. <https://doi.org/10.1101/658880>.
16. McKay, P.F., Zhou, J., Frise, R., Blakney, A.K., Bouton, C.R., Wang, Z., Hu, K., Samnuan, K., Brown, J.C., Kugathasan, R., et al. (2022). Polymer formulated self-amplifying RNA vaccine is partially protective against influenza virus infection in ferrets. *Oxf. Open Immunol.* 3, iqac004.
17. Pardi, N., Parkhouse, K., Kirkpatrick, E., McMahon, M., Zost, S.J., Mui, B.L., Tam, Y.K., Karikó, K., Barbosa, C.J., Madden, T.D., et al. (2018). Nucleoside-modified mRNA immunization elicits influenza virus hemagglutinin stalk-specific antibodies. *Nat. Commun.* 9, 3361.
18. Arevalo, C.P., Bolton, M.J., Le Sage, V., Ye, N., Furey, C., Muramatsu, H., Alameh, M.G., Pardi, N., Drapeau, E.M., Parkhouse, K., et al. (2022). A multivalent nucleoside-modified mRNA vaccine against all known influenza virus subtypes. *Science* 378, 899–904.
19. Lee, I.T., Nachbagauer, R., Ensz, D., Schwartz, H., Carmona, L., Schaefer, K., Avanesov, A., Stadlbauer, D., Henry, C., Chen, R., et al. (2023). Safety and Immunogenicity of a Quadrivalent, mRNA-based Seasonal Influenza Vaccine

- (MRNA-1010) in Adults: Interim Findings From a Phase 1/2 Randomized Clinical Trial. *Nat. Commun.* *14*, 3631.
20. Martínez-Orellana, P., Martorell, J., Vidaña, B., Majó, N., Martínez, J., Falcón, A., Rodríguez-Frandsen, A., Casas, I., Pozo, F., García-Migura, L., et al. (2015). Clinical response to pandemic h1n1 influenza virus from a fatal and mild case in ferrets Influenza viruses. *Virology* *12*, 48.
 21. Münzebrock, K., Pontes, A., Ho, F.Y., Garcia, J., Rip, J., and Creemers, L. (2023). Poly(Amido Amine) Nanoparticles Enable Mrna Delivery Into Cells Of Human Cartilaginous Tissues. *Osteoarthritis Cartilage* *31*, S221–S222.
 22. Lin, C., Zhong, Z., Lok, M.C., Jiang, X., Hennink, W.E., Feijen, J., and Engbersen, J.F.J. (2007). Novel bioreducible poly(amido amine)s for highly efficient gene delivery. *Bioconjug. Chem.* *18*, 138–145.
 23. Natarajan, J.K., Alumasa, J.N., Yearick, K., Ekoue-Kovi, K.A., Casabianca, L.B., de Dios, A.C., Wolf, C., and Roepe, P.D. (2008). 4-N-4-S-and 4-O-chloroquine analogues: Influence of side chain length and quinolyl nitrogen pKa on activity vs chloroquine resistant malaria. *J. Med. Chem.* *51*, 3466–3479.
 24. Liu, S.T.H., Behzadi, M.A., Sun, W., Freyn, A.W., Liu, W.C., Broecker, F., Albrecht, R.A., Bouvier, N.M., Simon, V., Nachbagauer, R., et al. (2018). Antigenic sites in influenza H1 hemagglutinin display species-specific immunodominance. *J. Clin. Invest.* *128*, 4992–4996.
 25. Madeira, F., Pearce, M., Tivey, A.R.N., Basutkar, P., Lee, J., Edbali, O., Madhusoodanan, N., Kolesnikov, A., and Lopez, R. (2022). Search and sequence analysis tools services from EMBL-EBI in 2022. *Nucleic Acids Res.* *50*, W276–W279.

OMTN, Volume 35

Supplemental information

Polymeric nanoparticle-based mRNA

vaccine is protective against

influenza virus infection in ferrets

Gijs Hardenberg, Chantal Brouwer, Rachelle van Gemerden, Nicola J. Jones, Anthony C. Marriott, and Jaap Rip

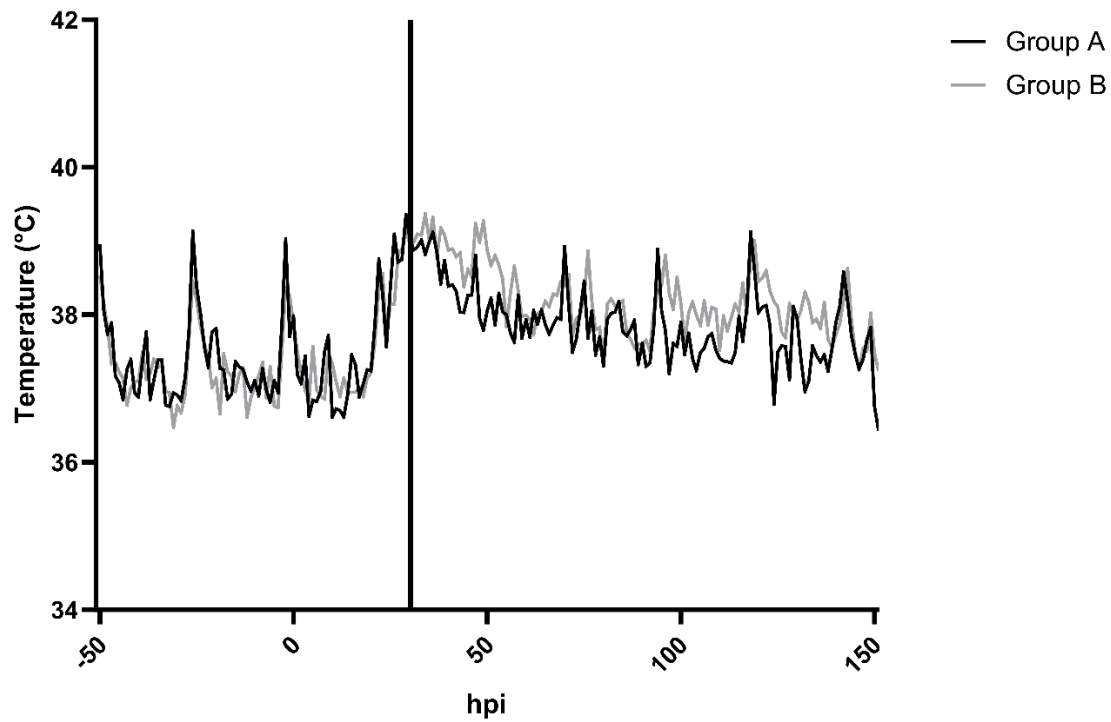


Figure S1. Group mean temperatures from data loggers

Group mean temperatures were calculated without normalising to the baseline. Lines show group mean temperatures of group A and group B. Ferrets were infected at 0 hpi (vertical line). The 24-hour cycling in temperature which can be seen prior to infection, was not resumed for either group until approximately 170 hours (7 days) post-infection (hpi).

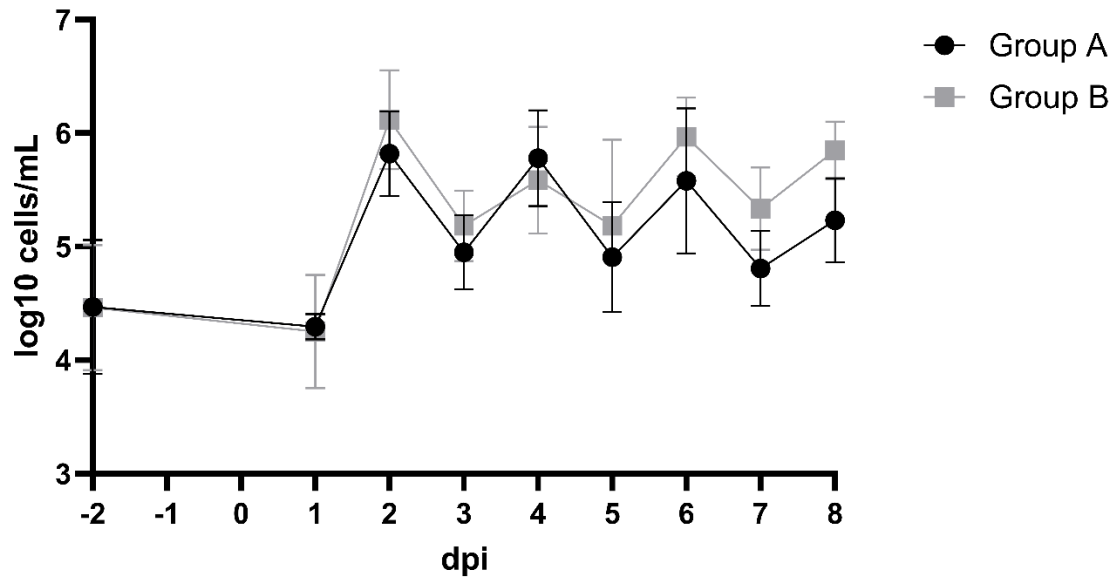


Figure S2. Nasal wash cell counts

Nasal wash viable cell counts were taken two days prior to challenge for a baseline and for eight days following GM19 challenge. The data was log-transformed and mean and standard deviation were plotted. No differences between group A and group B animals could be detected. dpi = days post infection.

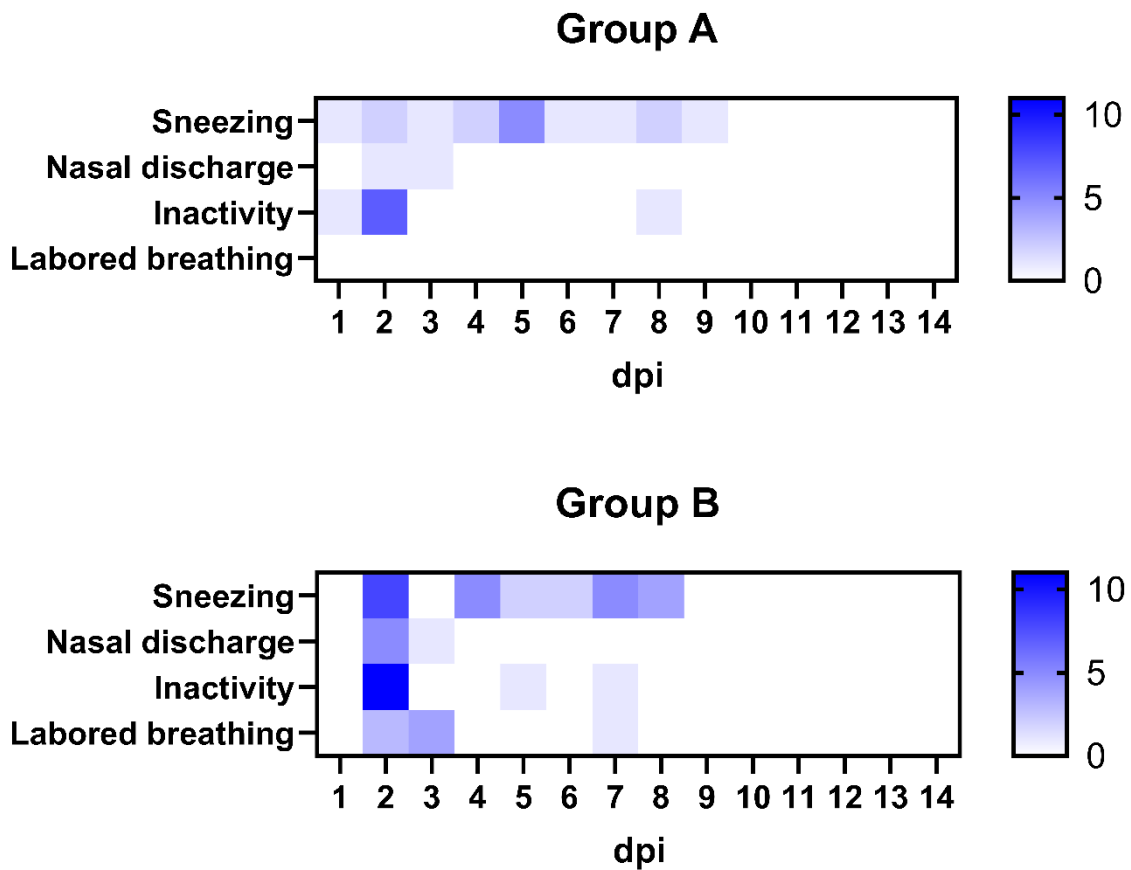


Figure S3. Clinical signs as heat map

Time-course of clinical signs shown as heat maps. For each day, the instances of each sign were summed for group A and group B and plotted. Shades indicate the occurrences per group, with darker shades indicating higher number of occurrences and lighter shades indicating lower number of occurrences per group (see legend next to heat map). dpi = days post infection.

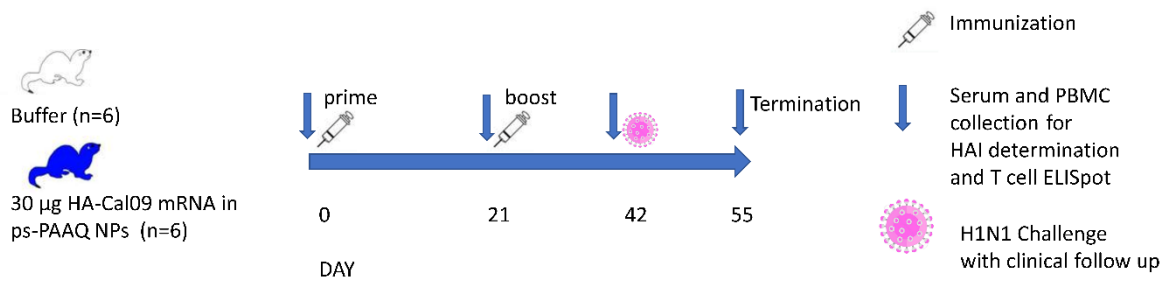


Figure S4. Treatment schedule

Graphical representation of treatment schedule.

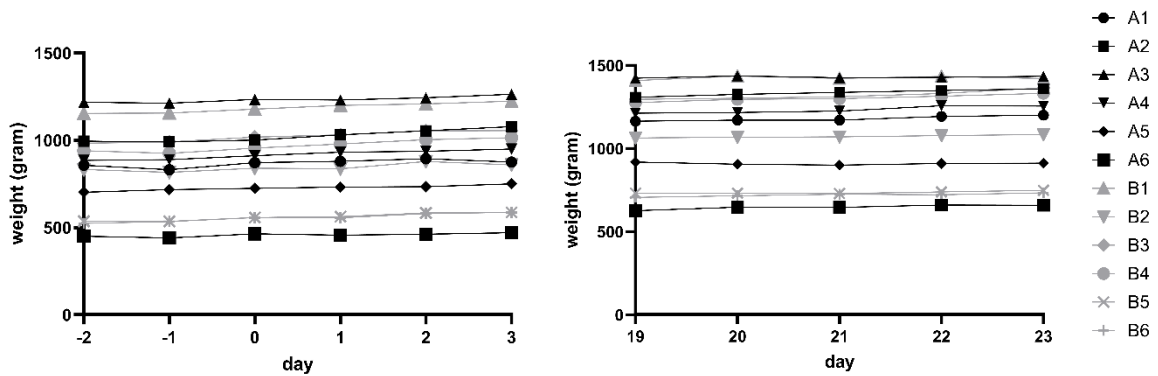
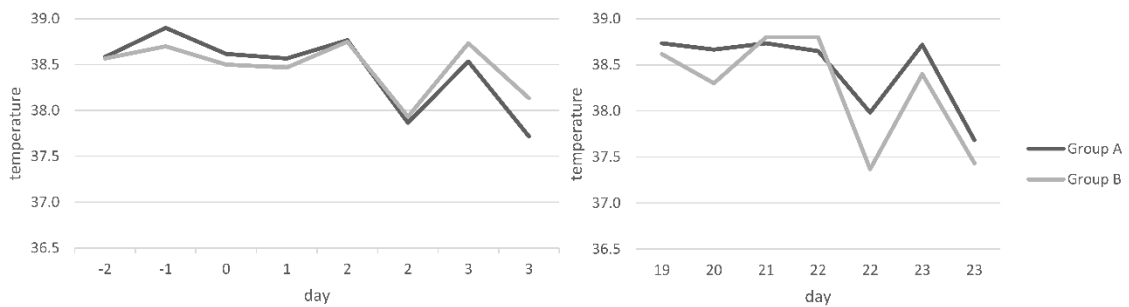
A**B**

Figure S5. Body weight and temperature after vaccination

Body weight (A) and temperature (B) measured following primary and booster vaccination.

For body weights individual animals are shown (A1-A6 (group A) are vaccinated animals and animals B1-6 (group B) received buffer). For temperature, group mean temperatures are depicted. On day 2, 3, 22 and 23 temperature measurements were performed in the morning and afternoon.